https://doi.org/10.33271/nvngu/2022-3/037

N. V. Morkun,
orcid.org/0000-0002-1261-1170,
V. V. Tron,
orcid.org/0000-0002-6149-5794,
O. Y. Serdiuk,
orcid.org/0000-0003-1244-7689,
A. A. Haponenko,
orcid.org/0000-0003-1128-5163

Kryvyi Rih National University, Kryvyi Rih, Ukraine, e-mail: nmorkun@gmail.com

COMPLEX MEASUREMENT OF PARAMETERS OF IRON ORE MAGNETIC SEPARATION BASED ON ULTRASONIC METHODS

Purpose. To develop a method for complex ultrasonic measurement of such parameters of the iron ore slurry flow passing through the working chamber of the magnetic separator as efficiency, concentration and grade size distribution of solid-phase particles.

Methodology. The research uses methods of modelling processes of ultrasonic wave propagation in the iron ore slurry. Ultrasonic wave absorption and scattering in water with solid particles and air bubbles are considered. To characterize absorption and scattering of acoustic oscillations by oscillating gas bubbles, concepts of effective cross-sections of attenuation, absorption and scattering are introduced.

Findings. The dependence of the phase velocity of asymmetric Lamb waves on the wall thickness of the magnetic separator was obtained. As a result of computer simulation of the process of ultrasonic waves propagation, its time and frequency characteristics were obtained. Based on the data obtained using ultrasonic measurements, the coefficients of the Rozin-Rammler equation for the characteristics of the ore material at various points of the technological line were calculated.

Originality. The proposed method of ultrasonic measurement of characteristics of the iron ore slurry in the working chamber of the magnetic separator differs from the existing ones in the fact that the Lamb wave source operates in a wide pattern and is connected by a V-shaped scheme which makes it possible to create a beam of coherent waves propagating both in the container wall (the working separator chamber) and in the measured medium (the iron ore slurry).

Practical value. The practical value consists in developing an ultrasonic measuring channel scheme for determining characteristics of the iron ore slurry in the working chamber of the magnetic separator.

Keywords: *ultrasound, measurement, iron ore slurry, magnetic separator*

Introduction. In processing iron ore raw materials, characteristics of technological flows between technological operations are monitored [1, 2]. These parameters include flow efficiency, solids concentration and grade size distribution. At the same time, control of these parameters in the working containers of technological units is a complex task. It should be noted that the potential to control parameters of the material flow inside the magnetic separator in different working conditions allows selecting the optimal operation mode and increasing both efficiency of the separator and the end product quality.

Literature review. Wet magnetic separation is characterized by the following main parameters: efficiency, waste rock content in the concentrate, magnetic material losses in tailings and total water consumption during the process [3]. At the same time, there is a large number of mode parameters that influence operation of the magnetic separator. In [4], such parameters as the rate of the magnetic material feed, content of the magnetic material in the ore material, concentration of solid-phase particles, the design of the magnetic separator unit and that of the separator container are considered. Also, the separator efficiency is influenced by such parameters as the slurry level in the separator, the angle of the magnetic unit, clearances between the drum and the container and the drum rotation speed.

Research [5] reveals that the main mechanism of obtaining fine-grained magnetite particles is magnetic flocculation in the separator's working container. In order to implement flocculation, it is necessary to maintain sufficiently high concentration of the magnetic material in the separator feed.

When processing coarser materials, the solids flow rate is the factor that requires reduction of the solid-phase slurry output [3]. When the ore material reduces in grade size due to the removal of waste rock by chains of ferromagnetic particles, shearing of waste rock particles into the concentrate increases. It should be noted that if ore particles are sufficiently fine, waste rock particles tend to act as part of the fluid medium and a significant portion of them is extracted into the concentrate along with water.

The amount of ore materials inside the separator is an important factor that affects the solids concentration in the concentrate and its quality [3]. The accumulated material is significantly influenced by the following separator parameters. First, the angle of the magnetic unit which determines the height to which the separator drum lifts the magnetic material when discharging the concentrate: the greater the mentioned height is, the more effective removal of the material is and the less material accumulates in the dehydrated area. Second, the drum rotation speed: the higher the speed is, the less time for the water to drain is needed. Third, the distance between the overflow drain and the separator drum is important as well.

Ultrasonic nondestructive testing methods are applied to measure the above parameters of the magnetic separator making it a promising trend.

To measure the fluid (slurry) flow rate using ultrasound, the following methods are applied [6]: phase, frequency, and time-pulse. The ultrasonic flow-meter operation is based on shearing ultrasonic oscillations passing through the moving fluid medium [7].

The phase method is based on the process of forming two ultrasonic oscillations directed along the fluid flow and against it followed up by measuring a phase difference of these oscillations [6, 8]. The disadvantage of this method is the need to use four piezo-element pairs instead of two, this making the design more expensive. Another disadvantage is the mortise method of installation [9].

The frequency method involves pulse modulation of ultrasonic oscillations with subsequent measurement of their frequencies. These ultrasonic oscillations are formed simultaneously along the medium flow and against the movement, the difference in their frequencies being proportionate to the fluid flow rate [6].

The time-pulse method is based on the fact that the propagation velocity of sound waves in the moving medium is equal to the vector sum of the sound velocity in the stationary medium and the medium velocity [6, 10].

To improve accuracy of the time-pulse method, two measurement channels are used with the fluid flow movement increasing the ultrasound velocity in one direction and reducing it in the other by an order of magnitude respectively [6].

[11] suggests an approach to measuring the fluid rate. This approach is based on the dependence of the flow velocity of the measured medium on the time difference of short ultrasonic pulses movement. These pulses are generated both in the direction of flow movement of the measured medium and against it. At that, primary ultrasonic transducers operate in two modes of radiation patterns – narrow and wide ones.

When forming the narrow radiation pattern, Rayleigh surface ultrasonic waves are used. This mode is mainly applied to measuring the flow of pure fluid media [12].

The wide pattern is formed by using Lamb waves. Waves of this type are generated and propagate in the pipe wall and also in the flow of the measured medium. Thus, they create a beam of coherent rays that covers a significant part of the flow [10, 13]. The advantage of this method is its resistance to contamination of the measured medium.

In [3, 14], the method of acoustic backscattering is proposed to study the above processes in the magnetic separator. The approach is based on the ultrasonic velocity profiling method for measuring the slurry particle velocity and short-term evaluation of power spectral density to obtain information on concentration of solid-phase particles. The first method, ultrasonic velocity profiling, is the ultrasonic echo-pulse method of measuring particle velocity [15, 16]. For arbitrary directed measurements in a two-dimensional plane, the results of two simultaneous measurements are combined. The advantage of this method is high spatial resolution and a discrete sampling rate. The second method, short-term evaluation of power spectral density, implies radiation of ultrasonic pulses into the slurry and recording of the resultant backscattering.

Research [17] presents the results of studying piezoelectric active sensors for excitation and detection of Lamb waves. The model presented in this paper uses the Fourier transform in the spatial domain. A general solution for the generalized expression for shear-stress distribution on the media boundary is obtained and reduced to the closed-form expression form for the ideal coupling case.

Research [18] considers a classical one-dimensional analysis of piezoelectric active sensors. An analytical model based on the theory of structural oscillations and the theory of piezoelectric transducers for predicting the electromechanical impedance response to be measured at the piezoelectric transducer leads is presented. The response of the structure is proven not to be altered by the transducer available, this fact confirming its non-invasive characteristics.

Purpose. The research is aimed at developing a method for ultrasonic measurements of the following parameters of the iron ore slurry flow passing through the working chamber of the magnetic separator:

- efficiency;
- fraction of solid-phase particles;
- grade size distribution of solid-phase particles under the wide radiation pattern of the Lamb wave source, which is connected by the V-shaped scheme to create a beam of coherent waves propagating both in the container wall (the separator's working chamber) and in the measured medium (the iron ore slurry).

Methods. Viscosity and thermal conductivity of the medium cause irreversible losses of ultrasonic wave energy [19].

Research [11] suggests mathematical description of the dependence of the medium flow on the difference of ultrasonic signals propagation time along the slurry flow and against it

$$v = \frac{\Delta t c_0^2}{2 L_a \cos\alpha},$$

where c_0 is the ultrasonic signal velocity in the stationary measured medium; L_a is the length of the active part of the acoustic channel.

It should be noted that the study on attenuation and scattering of ultrasonic wave energy is complicated by solid-phase particles and gas bubbles available in the medium. When the wavelength λ is commensurate with the size of the solid-phase particles, the degree of wave scattering becomes significant. With a large number of chaotically arranged solid-phase particles, scattering occurs in different directions. As a result, when determining the total ultrasonic wave intensity in a particular point of the medium, it is necessary to calculate the sum of wave intensities reflected from all the particles. In this case, the values of scattering cross-sections are additive, this resulting in the following dependences of linear coefficients of absorption $\Sigma_c(\lambda)$ and scattering $\Sigma_S(\lambda)$

$$\Sigma_c(\lambda) = n\sigma_c(\lambda);$$
$$\Sigma_S(\lambda) = n\sigma_S(\lambda), \quad (1)$$

where n is concentration of the solid-phase particles in the measured medium; $\sigma_c(\lambda)$ is the full absorption cross-section of the ultrasonic wave; $\sigma(\lambda)$ is the full scattering cross-section of the ultrasonic wave.

It should be noted that the values of the total absorption and scattering cross-sections in (1) are significantly influenced by the wavelength of the ultrasonic signal, as well as the size of solid-phase particles.

Based on the kinematic equation, the main characteristic of the ultrasonic radiation field $I_\lambda(\vec{r},\vec{\Omega})$ can be calculated. To write the equation of ultrasonic field characteristic, it is necessary to set the scattering coefficient value

$$\Sigma_S(\vec{\Omega}\to\vec{\Omega}') = n\sigma_S(\vec{\Omega}\to\vec{\Omega}'),$$

where $\sigma_S(\vec{\Omega}\to\vec{\Omega}')$ is the value of the energy scattering cross-section on the solid-phase particle. This value $\sigma_S(\vec{\Omega}\to\vec{\Omega}')d\vec{\Omega}'$ defines part of the energy scattered by the particle into the solid angle characterized by the value $d\vec{\Omega}'$. To determine the total scattering cross-section σs based on the value of the differential scattering cross-section, the following formula is applied

$$\sigma_S = \int_{4\pi} \sigma_S(\vec{\Omega}\to\vec{\Omega}')d\vec{\Omega}'.$$

On the basis of the energy balance equation in the elementary volume of the phase space, let us express the kinetics equation the solution of which results in the function $I_\lambda(\vec{r},\vec{\Omega})$

$$\vec{\Omega}\nabla I_\lambda(\vec{r},\vec{\Omega}) = -\Sigma(\lambda)I_\lambda(\vec{r},\vec{\Omega}) + \int d\Omega'\Sigma_S(\vec{\Omega}'\to\vec{\Omega})I_\lambda(\vec{r},\vec{\Omega}') + S_\lambda(\vec{r},\vec{\Omega}), \quad (2)$$

where $\Sigma(\lambda) = \Sigma\_(\lambda) + \Sigma_S(\lambda)$. $S_\lambda(\vec{r},\vec{\Omega})$ is the value of radiation density of the ultrasonic source. Let us reduce expression (2) to the integral representation

$$I_\lambda(\vec{r},\vec{\Omega}) + \int d\vec{r}' \int d\vec{\Omega} \sum_s (\vec{\Omega}' - \vec{\Omega}) \frac{e^{-\tau(\vec{r}',\vec{r},\lambda)}}{\left(\vec{r} - \vec{r}'\right(} \times$$
$$\times \delta\left[\vec{\Omega} - \frac{(\vec{r} - \vec{r}')}{\left(\vec{r} - \vec{r}'\right(}\right] I_\lambda(\vec{r}',\vec{\Omega}') + I_\lambda^0(\vec{r},\vec{\Omega}) \quad (3)$$

where $\tau(\vec{r}',\vec{r},\lambda) = \Sigma(\lambda)|\vec{r} - \vec{r}'|$, $\delta(\cdot)$ is the Dirac delta-function; $I_\lambda^\circ(\vec{r},\vec{\Omega}) = \int_0^\infty S_\lambda(\vec{r} - \xi\vec{\Omega},\vec{\Omega}) e^{-\tau(\xi,\lambda)} d\xi$ is the intensity of the non-scattered ultrasonic wave; $\xi = |\vec{r} - \vec{r}'|$. By decomposing the solution by multiplicity of ultrasonic wave scattering, we can write it in the form of the Neumann series [20]. In this decomposition, the first term defines the non-scattered ultrasonic radiation field, the second term defines the single-fold scattered radiation, the third term defines the twofold scattered radiation, etc.

Since the procedure for obtaining an analytical solution is already unsolvable in case of single-fold scattering, it is reasonable to use methods for numerical solution of integral equation (3), e.g. the Monte Carlo method [12].

Ultrasonic waves attenuate in water in the presence of solid particles and air bubbles mainly due to absorption and scattering of wave energy on particles and bubbles [19]. To theoretically investigate into ultrasound propagation, it is necessary to know the corresponding absorption and scattering cross-sections.

Suppose that there are spherical solid particles of the radius r and density ρ_1 in water, then the absorption cross-section on such particles, as shown in the works by L. Bergman, will be defined by the formula

$$\sigma_c(\lambda) = \frac{4\pi r^3}{3} \hbar \left(\frac{\rho_1}{\rho_\circ} - 1\right)^2 \frac{S}{S^2 + (\rho_1/\rho_0 + \tau)^2}, \quad (4)$$

where $\hbar = 2\pi/\lambda$ is a wave number, ρ_0 is fluid density; $S = \frac{9}{4Br}\left(1 + \frac{1}{Br}\right)$; $B = (\pi\nu/\mu)^{\frac{1}{2}}$; $\tau = \frac{1}{2} + \frac{9}{4Br}$; $\mu = \eta/\rho_0$; η is the fluid viscosity coefficient; ν is ultrasound frequency.

The absorption cross-section in (4) defines the fraction of energy absorbed by a particle. The energy losses occur due to friction (viscosity) during particle oscillations.

Diffraction caused by heterogeneity in the medium (suspended particles) results in sound wave energy scattering. The cross-section of this process is defined by the expression

$$\sigma_S(\lambda) = \frac{4\pi}{3} \cdot r^3 \cdot \frac{1}{6} k^4 \cdot r^3, \quad (5)$$

where k is a wave number; r is the particle radius.

It is revealed in (5) that $\sigma_S(\lambda) \sim \frac{1}{\lambda^4}$, so with increased frequency the scattering cross-section increases $(\sigma_S) \sim \nu^4$.

Fig. 1 reveals dependences of ultrasound absorption, scattering and attenuation cross-sections on solid-phase particles in water on frequency of acoustic oscillations. The particle radius is 0.01 cm. As can be seen from Fig. 1, ultrasonic scattering becomes substantial when the wavelength l of acoustic oscillations is commensurate with the particle size.

Gas bubbles available in the fluid make sound energy be absorbed and scattered. However, unlike on solid-phase particles, absorption and scattering on gas bubbles is of resonant character.

The main reasons for this phenomenon are as follows:

a) heating of the bubble and heat removal to the fluid by periodic changes in the bubble volume which it experiences under the action of the sound wave;

b) scattering of part of the sound energy because the oscillating bubble is a spherical sound radiator;

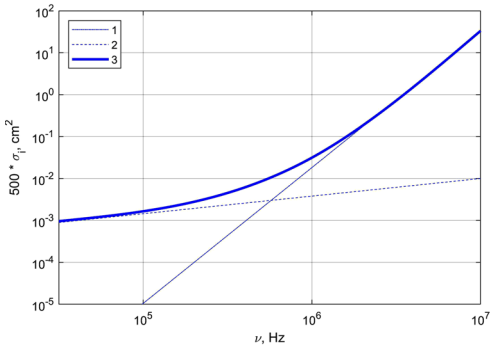

Fig. 1. Dependence of ultrasound absorption and scattering cross-sections on suspended particles on frequency of oscillations:
1 – σ_s – scattering cross-section; 2 – σ_c – absorption cross-section, the particle radius is $\vec{r} = 0.01$ cm

c) energy losses due to formation of fluid flows around the oscillating bubble.

To characterize absorption and scattering of acoustic oscillations by oscillating gas bubbles, notions of effective cross-sections of attenuation σ_p, absorption σ_c, and scattering σ_s are introduced. The effective attenuation cross-section σ_p refers to the cross-section area perpendicular to the sound wave incidence for which the incoming sound energy is equal to total energies absorbed and scattered by the bubble.

Absorption and scattering cross-sections of air bubbles are determined by the formulas

$$\sigma_c = \frac{4\pi R^2(\delta/\eta - 1)}{(\nu_0^2/\nu^2 - 1)^2 + \delta^2}; \quad \sigma_S = \frac{4\pi R^2(\delta/\eta)}{(\nu_0^2/\nu^2 - 1)^2 + \delta}, \quad (6)$$

where ν_0 is the resonant frequency of the bubble of the radius R; δ is the attenuation constant;

$$\eta = 2\pi R/\lambda.$$

Analysis of formulas (6) reveals the maximum values of cross-sections achieved at $\nu = \nu_0$.

The total attenuation cross-section is determined by the sum of absorption and scattering cross-sections

$$\sigma_p = \sigma_c + \sigma_S = \frac{4\pi R^2}{(\nu_0^2/\nu^2 - 1)^2 + \delta}.$$

The value of resonant frequency of air bubbles in water can be evaluated by the formula

$$\nu_0 R = 0.328 \cdot 10^3.$$

The value of the attenuation constant depends on the sound frequency and varies from 0.08 to 0.013 within the frequency interval from 20 to 1000 kHz [23].

Since sound energy absorption and scattering on air bubbles is resonant, in order to calculate ultrasonic wave attenuation by air bubbles, it is necessary to know not only the corresponding attenuation-cross sections, but also the grade size distribution function of air bubbles.

Let us denote the bubble size distribution function by $f(R)$. Then the value dR conditions the fraction of bubbles of sizes within R to $R + dR$.

The specific values of the air volume fraction in water and the gas bubble size distribution function are selected according to the research results presented in in the works by V. A. Nosov.

The value of the signal S_1 measured at the volumetric ultrasonic frequency of $\nu \geq 5$ MHz is determined by two parameters – solid phase concentration and its particle size distribution [4]

$$S_1 = \ln \frac{I_o}{\langle I_\nu(Z) \rangle}, \quad (7)$$

where $\langle I_\nu(Z) \rangle$ is the mean wave intensity.

It is reasonable to apply Lamb waves to obtaining the value proportionate to the solid phase concentration only [28].

The intensity of Lamb waves at the distance l from the wave source can be determined by the formula [28]

$$I_{l,\nu} = I^*_{l,\nu} \exp\left\{-W\frac{[\rho_p - \rho_w]}{\rho}C_\nu l\right\}, \quad (8)$$

where ρ_p is density of ore particles; ρ_w is water density. As is seen from (8), the signal

$$S_2 = \ln\left(\frac{I^*_{l,\nu}}{I_{l,\nu}}\right) = W\frac{[\rho_p - \rho_w]C_\nu l}{\rho}, \quad (9)$$

is proportionate to the volume fraction of solid-phase particles in the slurry W. It should be noted that this value does not depend on availability and the number of gas bubbles in the measured medium.

Thus, it is reasonable to apply the value of quotient S_1 from expression (7) and S_2 from expression (9) to characterizing grain size distribution of the iron-ore slurry

$$S = \frac{S_1}{S_2} = \frac{Z\rho}{lC_\nu \aleph(\rho_p - \rho_w)}\int_0^{r_m}\sigma(v,r)F(r)dr. \quad (10)$$

The value S is determined solely by the solid-phase particle size of the slurry, i. e. it unambiguously determines concentration of the control grade size.

The particle grade size distribution function $F(r)$ can determine the content of particles of a particular size $\omega_{\pm r}$

$$\omega_{-r} = \frac{4}{3}\pi\int_{\circ}^{r} r^3F(r)dr \Big/ \aleph, \quad (11)$$

where $\aleph = \frac{4}{3}\pi\int_o^{r_m} r^3F(r)dr$.

To obtain lognormal distribution $F(r)$, the mean particle size $\langle R\rangle$ is the main parameter which also determines concentration ω_{-r}. As can be seen from expressions (10) and (11), there is a one-valued correspondence between ω_{-r} and S as both values are determined by the same particle size distribution law $F(r)$. Fig. 2 shows curves establishing the correspondence between ω_{-r} and S for different grades.

Thus, the method described above enables determining solid phase concentration and the content of the ground material of several grade sizes. These measurements do not require slurry pre-degassing.

Findings. The scheme in Fig. 3, *a* is proposed to implement the method of complex ultrasonic measurement of parameters of the iron-ore slurry flow passing through the working chamber of the magnetic separator, namely efficiency, fraction of solid-phase particles, prevailing grade size of the solid phase. In accordance with this scheme, the source of Lamb waves operates under the wide radiation pattern and is connected in a V–shaped scheme (Fig. 3, *b*) to create a beam of coherent waves propagating both in the container wall (the separator's working chamber) and in the measured medium (the iron ore slurry).

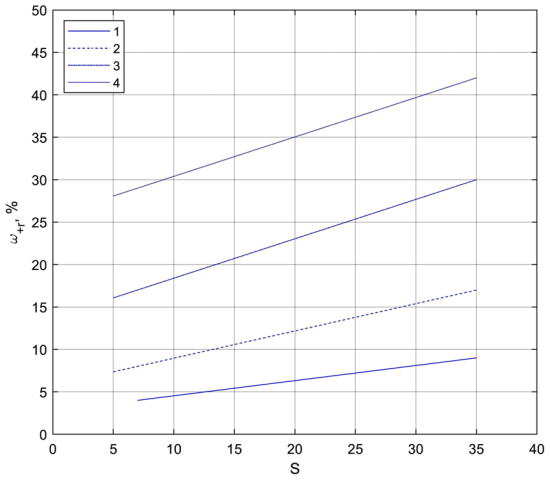

Fig. 2. Curves for different grades:
1 – r = 44 μm; *2 – r* = 60 μm; *3 – r* = 74 μm; *4 – r* = 50 μm

There are various ways to excite Lamb waves [19, 20], but the wedge method is the most common (Fig. 4). Lamb waves excited in plates can have different orders (modes). In order to excite waves of the desired order with minimal amplitude of other order waves, the wedge angle q (Fig. 4) should be determined from the ratio

$$\theta = \arcsin(C^{cl}/C_n), \quad (12)$$

where C^{cl} is the longitudinal wave velocity in the wedge material; C_n is the velocity of n^{th}-order Lamb wave propagation in the plate.

The wedge method is normally used to excite either a symmetric or an antisymmetric zero-order Lamb wave. To determine the wedge angle in this case, one needs to know the corresponding Lamb wave velocities in the plate. Let us denote the wave number of zero-order Lamb waves by $K(K = (2\pi\nu)/C)$.

As follows from the works by I. A. Viktorov, characteristic equations defining eigenvalues of the wave number K have the form

$$(K^2 + s^2)\,\mathrm{ch}\,(qd)\,\mathrm{sh}\,(sd) - 4K^2qs\,\mathrm{sh}(qd)\,\mathrm{ch}\,(sd) = 0;$$

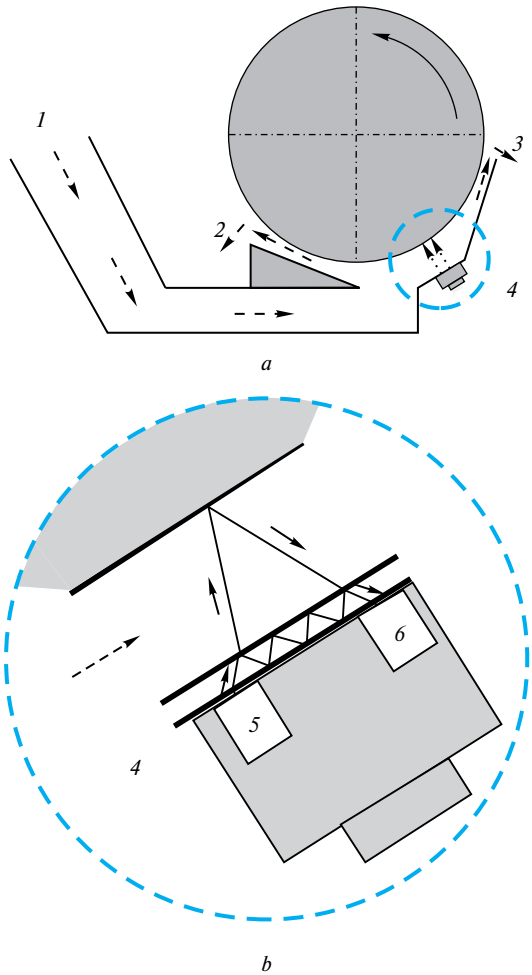

Fig. 3. Complex ultrasonic measurement of iron ore slurry flow parameters:
1 – slurry flow; 2 – non-magnetic product; 3 – magnetic product; 4 – ultrasonic measuring channel; 5 – ultrasonic source; 6 – ultrasonic receiver

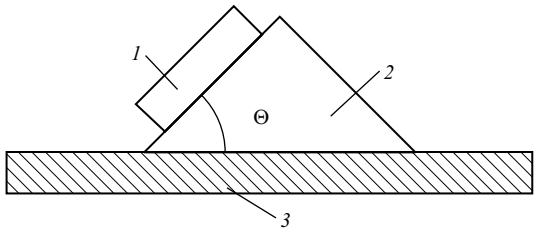

Fig. 4. Location of the piezoelectric radiator on the measurement plate:
1 – radiator; 2 – shaping prism; 3 – plate

$$(K^2 + s^2)\,\mathrm{sh}(qd)\,\mathrm{ch}(sd) - 4K^2 qs\,\mathrm{ch}(qd)\,\mathrm{sh}(sd) = 0, \quad (13)$$

where d is thickness of the plate; $s = \sqrt{K^2 - K_t^2}$; $q = \sqrt{K^2 - K_l^2}$; K_l and K_t are longitudinal and shear wave numbers determined through the corresponding velocities C_l and C_t of longitudinal and shear waves in the plate material

The phase velocity of Lamb waves C is found by numerical solution of characteristic equations (13), which for these calculations are convenient to be rewritten in the dimensionless form for symmetric waves

$$\frac{\mathrm{tg}\left[\sqrt{1-\mu^2}\,\bar{d}\right]}{\mathrm{tg}\left[\sqrt{\xi^2-\mu^2}\,\bar{d}\right]} = -\frac{4\mu^2\sqrt{\xi^2-\mu^2}\sqrt{1-\mu^2}}{\left(2\mu^2-1\right)^2},$$

for antisymmetric waves

$$\frac{\mathrm{tg}\left[\sqrt{1-\mu^2}\,\bar{d}\right]}{\mathrm{tg}\left[\sqrt{\xi^2-\mu^2}\,\bar{d}\right]} = -\frac{\left(2\mu^2-1\right)^2}{4\mu^2\sqrt{\xi^2-\mu^2}\sqrt{1-\mu^2}}, \quad (14)$$

where $\bar{d} = K_t d$; $\xi^2 = C_t^2/C_l^2$; $\mu^2 = C_t^2/C^2$.

Numerical solution of equation (14) is carried out by dividing the segment in half. The programme implementing the solution of this equation is given in [19].

Table 1 shows the results of C/C_t calculations for a steel plate

Fig. 5 presents a dependence of the phase velocity of antisymmetric Lamb waves on $\bar{d} = k_1 d$

The Lamb wave phase velocity values found in such a way allow evaluating the wedge angle according to formula (12). Table 2 presents the data on phase velocities for ultrasound frequency ν = 5MHz, wedge angles for plates of various thickness made of stainless steel 12X18H10T. The material of the wedge is Plexiglas.

The velocity of longitudinal waves in the wedge material (Plexiglas) is assumed to be equal to $C_l^w = 2670$ m/s.

According to the above scheme, the proposed method for complex ultrasonic measurement of parameters of the iron-ore slurry flow passing through the working chamber of the

Table 1

Results of C/C_t calculations

$\bar{d}$	0.25	0.50	1.00	1.25	1.50	2.0	3.0	5.0
C/C_1	0.063	0.164	0.461	0.611	0.717	0.820	0.887	0.918

Table 2

Calculation of the wedge angle ν = 5 MHz

d, mm	$\bar{d}$	C/C_t	C, m/s	q, deg.
0.5	4.99	0.916	2886	67.71
0.7	6.98	0.923	2905	66.77
1	9.98	0.924	2911	66.53
2	19.96	0.924	2911	66.53
3	29.93	0.924	2911	66.53

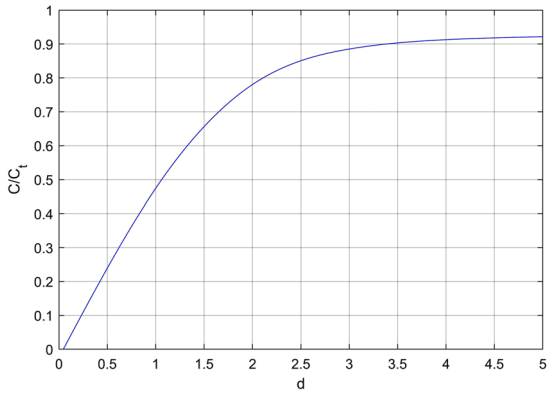

Fig. 5. Dependence of the phase velocity of antisymmetric Lamb waves on $\bar{d} = k_1 d$; d – thickness of the plate; k_1 – the shear wave number in the plate material (steel 12X18H10T)

magnetic separator, namely efficiency, fraction of solid-phase particles, the prevailing grade size of the solid phase is noted for operation of the Lamb wave source under the wide pattern. Connecting the source of ultrasonic waves by the V-shaped scheme creates a beam of coherent waves propagating in the container wall (the separator's working chamber), and in the measured medium (the iron ore slurry). As a result, the problem of dividing the received signal into the signal received from the container wall and that received from the iron ore slurry should be solved when receiving ultrasonic waves.

The specialized software package Waveform Revealer [13] is used to simulate ultrasonic wave propagation. The thickness of the magnetic separator wall in which ultrasonic waves propagate is 5mm. The software package Waveform Revealer allows simulation of multi-mode directional waves in thin plates. Piezoelectric wafer active sensors (PWAS) are used as signal receivers, Fig. 6.

The receiving transducer is placed at a distance of 10 cm from the ultrasonic wave source. The resulting signal is shown in Fig. 7.

Frequency characteristics of S_0 and A_0 trains are shown in Figs. 8–11.

The proposed method of ultrasonic measurements results in obtaining data on efficiency, fraction of solid-phase particles and grade size distribution of solids in the slurry to create a mathematical model of the process based on the Rosin-Rammler. The total yield of fractions is determined by the following formulas: for the fraction $r[d_1] - R[>d_1] = r[d_1]$; for the fraction $r[d_i] - R[>d_i] = r[d_1] + r[d_2] + \ldots r[d_i]$, for the fraction $r[d_m] - R[>d_m] = 1$. The following ore particle size fractions are considered during the research: +3, 3 + 1, 1 + 0.5, 0.5 + 0.25, 0.25 + + 0.125, 0.125 + 0.071, 0.071 + 0.056, 0.056 + 0.044, 0.044 + 0.

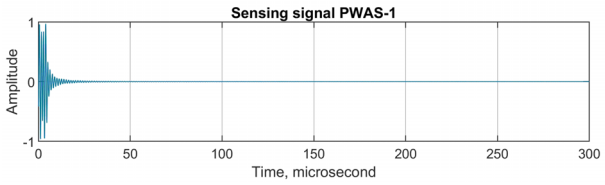

Fig. 6. Initial 5-period 5MHz signal of sinusoidal wave excitation

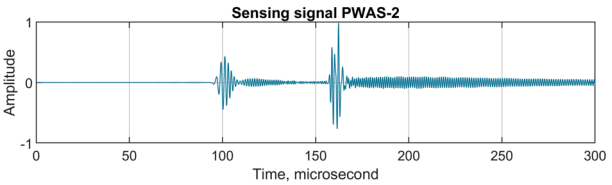

Fig. 7. Waveform of the received signal at 10 cm from the source

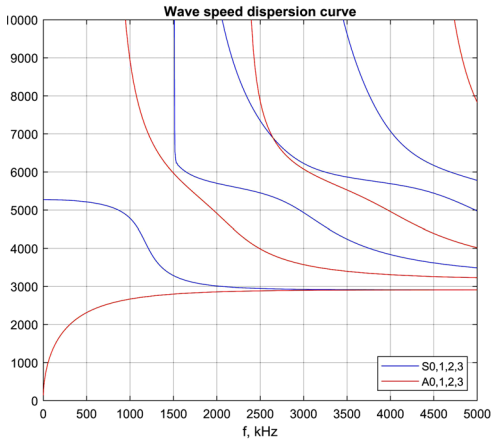

Fig. 8. Dispersion curves of the phase ultrasound velocity in a 5 mm thick steel plate

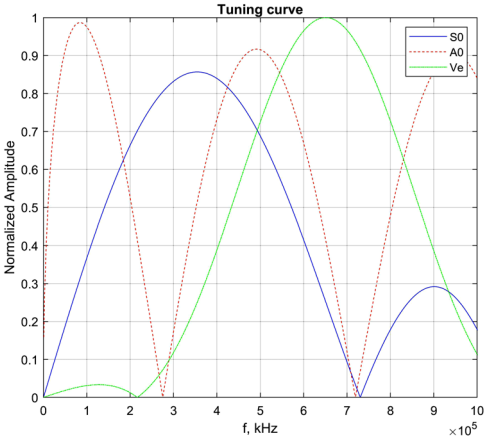

Fig. 9. Turning curve

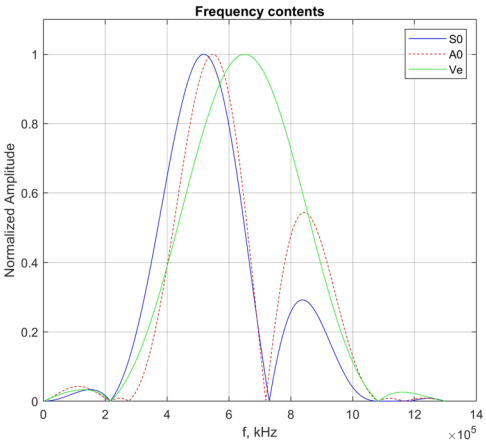

Fig. 10. Frequency of the wave train

The method proposed by prof. L. P. Shupov is applied to determining the Rosin-Rammler equation coefficients. The results of specifying the Rosin-Rammler equation coefficients to simulate distribution of ore particles by grade sizes are shown in Fig. 12.

Parameters of the Rosin-Rammler equation for characteristics of products at various process points are presented in Table 1.

To identify dependences that cannot be described analytically, it is appropriate to use a hybrid approach with fuzzy Takagi-Sugeno models.

Conclusions. Thus, the proposed method of complex ultrasonic measurement allows evaluating efficiency, solid-phase fraction and grade size distribution of solid-phase par-

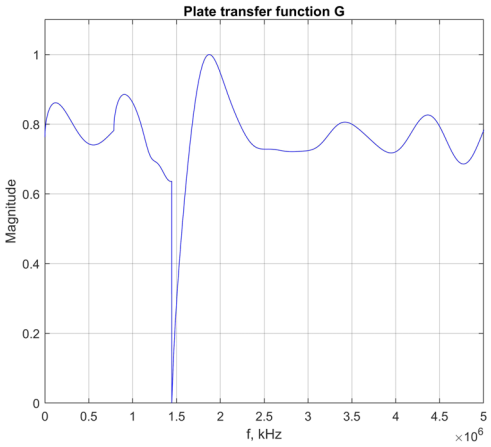

Fig. 11. Frequency of the wave propagation surface

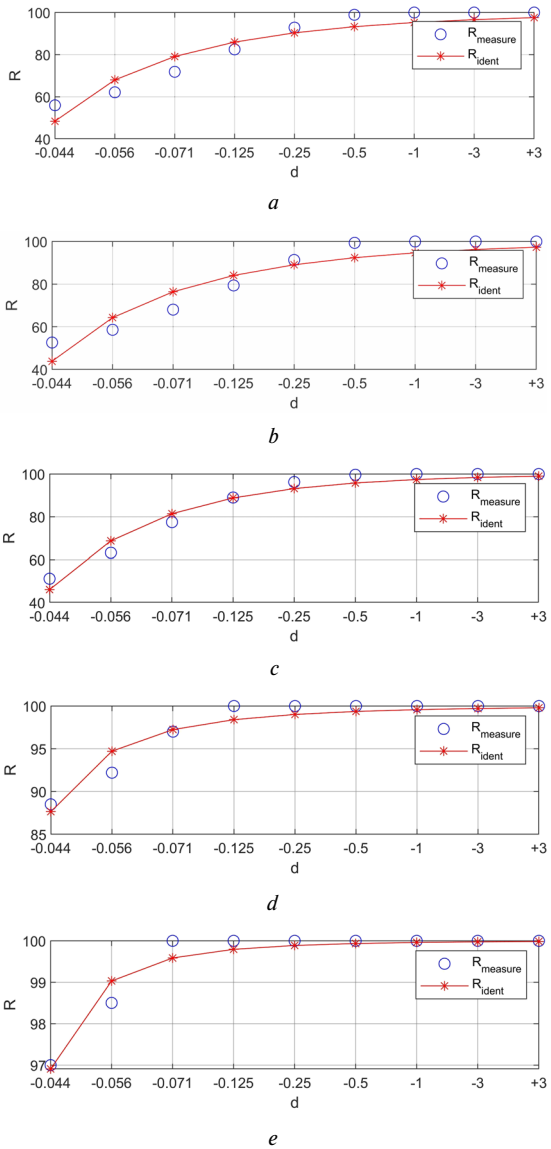

a

b

c

d

e

Fig. 12. Results of identifying parameters of the Rosin-Rammler equation:

a – the 1st-order magnetic product of the 1st-stage magnetic separation; b – the 2nd-order magnetic product of the 1st-stage separation; c – the 2nd-stage magnetic separation; d – the 3rd-stage magnetic separation product; e – the 4th-stage magnetic separation product

Table 3

Identification of Rosin-Rammler equation parameters

Process unit	A coeff.	a coeff.	Determination coeff.	Mean square error
1st-order 1st-stage magnetic separator	0.6612	0.7841	0.9054	5.7896
2nd-order 1st-stage magnetic separator	0.5767	0.8354	0.8972	6.5903
2nd-stage magnetic separator	0.6173	0.9121	0.9609	3.8813
3rd-stage magnetic separator	2.0908	0.4914	0.9224	1.2758
4th-stage magnetic separator	3.4752	0.4152	0.9418	0.2736

ticles in the iron ore slurry flow passing through the working chamber of the magnetic separator

References.

1. Stupnik, M., Kalinichenko, V., Pysmennyi, S., Kalinichenko, O., & Fedko, M. (2016). Method of simulating rock mass stability in laboratory conditions using equivalent materials. *Mining of Mineral Deposits*, *10*(3), 46-51. https://doi.org/10.15407/mining10.03.046.

2. Tkachov, V., Gruhler, G., Zaslavski, A., Bublikov, A., & Protsenko, S. (2018). Development of the algorithm for the automated synchronization of energy consumption by electric heaters under condition of limited energy resource. *Eastern-European Journal of Enterprise Technologies*, *2*(8(92)), 50-61. https://doi.org/10.15587/1729-4061.2018.126949.

3. Stener, J. F., Carlson, J. E., Palsson, B. I., & Sand, A. (2016). Direct measurement of internal material flow in a bench scale wet low-intensity magnetic separator. *Minerals Engineering*, *91*, 55-65. https://doi.org/10.1016/j.mineng.2015.10.021.

4. Morkun, V., & Morkun, N. (2018). Estimation of the crushed ore particles density in the pulp flow based on the dynamic effects of high-energy ultrasound. *Archives of Acoustics*, *43*(1), 61-67. https://doi.org/10.24425/118080.

5. Carrasco, C., Keeney, L., Napier-Munn, T.J., & Bode, P. (2017). Unlocking additional value by optimising comminution strategies to process Grade Engineering streams. *Minerals Engineering*, *103-104*, 2-10. https://doi.org/10.1016/j.mineng.2016.07.020.

6. Bondar, A. I., Degtyar, S. M., Pavlenko, S. A., Smolyakov, V. A., & Yudin, A.Y. (2010). Izmereniye raskhoda zhidkosti s pomoshchyu ultrazvukovogo raskhodomera. *Mekhaníka ta mashinobuduvannya*, *2*, 189-193.

7. Morkun, V., Morkun, N., & Pikilnyak, A. (2015). The study of volume ultrasonic waves propagation in the gas-containing iron ore pulp. *Ultrasonics*, *56*, 340-343. https://doi.org/10.1016/j.ultras.2014.08.022.

8. Morkun, V., Morkun, N., & Pikilnyak, A. (2014). Ultrasonic facilities for the ground materials characteristics control. *Metallurgical and Mining Industry*, *2*, 31-35.

9. Eyo, E. N., Pilario, K. E. S., Lao, L., & Falcone, G. (2021). Development of a real-time objective gas-liquid flow regime identifier using kernel methods. *IEEE Transactions on Cyberneticsthis*, *51*(5), 2688-2698. https://doi.org/10.1109/TCYB.2019.2910257.

10. Shi, J., Gourma, M., & Yeung, H. (2021). A CFD study on horizontal oil-water flow with high viscosity ratio. *Chemical Engineering Science*, *229*, 116097. https://doi.org/10.1016/j.ces.2020.116097.

11. Khlebnova, V. I. (2016). Methods and instruments for measuring the rate of liquids and gases: prospects of application of ultrasonic transducers with a wide measuring beam. *Proceedings of Higher Educational Institutions. Machine Building*, *9*(678), 45-52. https://doi.org/10.18698/0536-1044-2016-9-45-52.

12. Guo, P., Su, M., Cai, X., & Chen, L. (2015). Monte-Carlo simulation of multiple scattering of ultrasound by particles in liquid-solid two-phase flow. *Procedia Engineering*, *102*, 1373-1379. https://doi.org/10.1016/j.proeng.2015.01.269.

13. Splichal, J., & Hlinka, J. (2018). Modelling of health monitoring signals and detection areas for aerospace structures. *Proceedings of 13th Research and Education in Aircraft Design*, 170-188. https://doi.org/10.13164/conf.read.2018.17.

14. Wada, S., Tezuka, K., & Furuichi, N. (2013). Effect of low-frequency ultrasound on flow rate measurements using the ultrasonic velocity profile method. *Journal of Nuclear Science and Technology*, *50*(6), 654-663. https://doi.org/10.1080/00223131.2013.785269.

15. Tan, C., Murai, Y., Liu, W., Tasaka, Y., Dong, F., & Takeda, Y. (2021). Ultrasonic Doppler technique for application to multiphase flows: A Review. *International Journal of Multiphase Flow*, *144*, 103811. https://doi.org/10.1016/j.ijmultiphaseflow.2021.103811.

16. Nomura, S., De Cesare, G., Furuichi, M., Takeda, Y., & Sakaguchi, H. (2020). Quasi-stationary flow structure in turbidity currents. *International Journal of Sediment Research*, *35*(6), 659-665. https://doi.org/10.1016/j.ijsrc.2020.04.003.

17. Giurgiutiu, V. (2014). *Structural health monitoring with piezoelectric wafer active sensors*. Elsevier: Academic Press. https://doi.org/10.1016/C2013-0-00155-7.

18. Shen, Y., & Giurgiutiu, V. (2014). Predictive modeling of nonlinear wave propagation for structural health monitoring with piezoelectric wafer active sensors. *Journal of Intelligent Material Systems and Structures*, *25*(4), 506-520. https://doi.org/10.1177/1045389X13500572.

19. Morkun, V., Morkun, N., & Pikilnyak, A. (2014). The adaptive control for intensity of ultrasonic influence on iron ore pulp. *Metallurgical and Mining Industry*, *6*(6), 8-11.

20. Kirac, F., & Guven, O. (2015). Gamma radiation induced synthesis of poly(N-isopropylacrylamide) mediated by Reversible Addition–Fragmentation Chain Transfer process. *Radiation Physics and Chemistry*, *112*, 76-82. https://doi.org/10.1016/j.radphyschem.2015.03.013.

Комплексне вимірювання параметрів процесу магнітної сепарації залізорудної сировини на основі ультразвукових методів

Н. В. Моркун, В. В. Тронь, О. Ю. Сердюк, А. А. Гапоненко

Криворізький національний університет, м. Кривий Ріг, Україна, e-mail: nmorkun@gmail.com

Мета. Розроблення методу комплексного ультразвукового вимірювання параметрів потоку залізорудної пульпи, що проходить через робочу камеру магнітного сепаратора: продуктивності; концентрації частинок твердої фази; розподілу по крупності частинок твердої фази.

Методика. У роботі використані методи моделювання процесів поширення ультразвукових хвиль у залізорудній пульпи. Розглянуті процеси поглинання й розсіяння ультразвукових хвиль у воді за наявності твердих частинок і повітряних бульбашок. Для характеристики поглинання й розсіяння акустичних коливань газовою бульбашкою, введені поняття ефективних поперечних перерізів погашення, поглинання й розсіяння.

Результати. Одержана залежність фазової швидкості асиметричних хвиль Лемба від товщини стінки магнітного сепаратора. У результаті комп'ютерного моделювання процесу поширення ультразвукових хвиль одержані його часові й частотні характеристики. На основі даних, отриманих із використанням ультразвукових вимірювань, обчислені коефіцієнти рівняння Розіна-Раммлера для характеристик рудного матеріалу в різних точках технологічної лінії.

Наукова новизна. Пропонований метод ультразвукового вимірювання характеристик залізорудної пульпи в робочій камері магнітного сепаратора відрізняється від існуючих тим, що джерело хвиль Лемба працює в режимі широкої діаграми спрямованості й підключене за V-подібною схемою, що дозволяє створити пучок когерентних хвиль, які поширюються як у стінці ємності (робочої камери сепаратора), так і у вимірюваному середовищі (залізорудній пульпі).

Практична значимість. Полягає в розробленні схеми ультразвукового вимірювального каналу для визначення характеристик залізорудної пульпи в робочій камері магнітного сепаратора.

Ключові слова: *ультразвук, вимірювання, залізорудна пульпа, магнітний сепаратор*

The manuscript was submitted 30.08.21.